Damascus university journal
V… ( ): ??-??

مجلة جامعة دمشق للعلوم ....
المجلد ... العدد... : الصفحات.

Application of CineECG for Enhancing Cardiac Diagnosis: Review and Cases Study.

Mhd Jafar Mortada (MSc)[1], Agnese Sbrollini (PhD.)[2], Laura Burattini (Professor)* [3], Peter Van Dam (PhD)[4]

[1] PhD student. Università Politecnica delle Marche, Department of Information Engineering, m.j.mortada@pm.univpm.it.

[2] Postdoctoral research fellow, Università Politecnica delle Marche, Department of Information Engineering, a.sbrollini@staff.univpm.it.

[3] PhD Full Professor of Bioengineering, Università Politecnica delle Marche, Department of Information Engineering, l.burattini@staff.univpm.it.

[4] Researcher, ECG Excellence, peter.van.dam@peacs.nl.

Abstract:

Modern cardiology relies heavily on the standard resting 12-lead Electrocardiogram (ECG), as it provides information about the electrical functionality of the heart. However, performing diagnosing using ECG depends highly on the doctor's interpretations and understanding of its complex patterns. A technique based on Vectorcardiography method called CineECG, has been developed to provide a different representation of the ECG. In this study, we reviewed the CineECG method and described the equations behind it. Additionally, we tested the method on three cases, relating to healthy, left bundle branch block, and right bundle branch block subjects to verify the CineECG utility in the diagnostic process. Our results showed easily interpretable figures that can be used to aid in the diagnosis of these cases. Thus, CineECG represents a potentially useful tool for enhancing cardiac diagnosis.

Keywords: Electrocardiography, Vectorcardiography, CineECG, Left bundle branch block, right bundle branch block.

Received:
Accepted:

1. Introduction:

The Electrocardiogram, also known as ECG or EKG (from the German "Elektrokardiographie"), is a fundamental diagnostic tool in the field of cardiology. It provides valuable insights into the electrical activity of the heart, offering a window into its health and functionality, and with the right interpolation, ECG data can be used for early diagnosis of many heart malfunctions, such as blood clot(Thomson et al., 2019), ischemia(Wimmer et al., 2013), left bundle branch block (LBBB)(Sgarbossa, 2000) and right bundle branch block (RBBB)(Ikeda, 2021) just to name a few.

Despite its widely use, ECG interpretation is still very challenging and affected by intra- and inter-subject variability. Thus, automatic algorithms for the support of ECG interpretation are still desirable.

In this paper, we will review a novel way to look at the 12-leads ECG, called CineECG, introduced in 2022, the method aims to describe the path of the electrical activation during the heart cycle using the cardiac axis, and will test the algorithm on a normal case as well as clinical cases of LBBB and RBBB, which are two conduction disorders that effect the electrical path.

2. Electrocardiography and Vectorcardiography:

Standard 12-lead ECG is the most used type of ECG, it is composed of nine electrodes placed on the chest and limbs of the patient. Standard 12-lead ECG signals can be categorized into:

- Standard Limb Leads (I, II, III): also known as Einthoven triangle, offering a frontal plane view of the heart.
- Augmented Voltage Limb Leads (aVR, aVL, aVF): are derived from the standard limb leads and provide a view of the heart from different angles in the frontal plane.
- Precordial (Chest) Leads (V1-V6): which gives a transverse plane view of the heart.

As depicted in Figure (1), the 12 signals would describe the electrical activity of the heart from different angles, providing a complex understanding

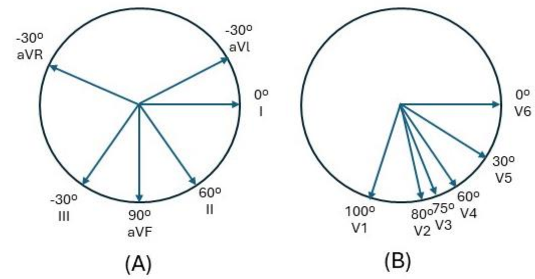

Figure 1 - Standard 12-leads ECG angles, (A) limb and augmented leads as seen in the frontal plane, (B) precordial leads as seen in axial plane.

of the path of the electrical signal through the structures of the heart. Because of the way it is composed, a redundancy in information exists, specifically in the augmented leads and the II, as shown in equations 1 to 4:

$$\mathrm{II}=\mathrm{I}+\mathrm{II} \tag{1}$$

$$\mathrm{aVL}=\mathrm{I}-\frac{\mathrm{II}}{2} \tag{2}$$

$$\mathrm{aVF}=\mathrm{II}-\frac{\mathrm{I}}{2} \tag{3}$$

$$\mathrm{aVR}=\frac{-(\mathrm{I}+\mathrm{II})}{2} \tag{4}$$

While these leads aim to describe a three-dimensional vector in space they are expressed as 2D signals, this leaded to the development of vectorcardiography or (VCG), a technique allows for the 3D visualization of the amplitude and direction of the heart activation, VCG can be calculated using Franks's leads(G Daniel et al., 2007; KORS et al., 1990), Equations 5 to 7.

$$VCG_x = -(-0.172\,V1 - 0.074\,V2 + 0.122\,V3 + 0.231\,V4 + 0.239\,V5 + 0.194\,V6 + 0.156\,I - 0.010\,II) \tag{5}$$

$$VCG_y = (0.057\,V1 - 0.019\,V2 - 0.106\,V3 - 0.022\,V4 + 0.041\,V5 + 0.048\,V6 - 0.227\,I + 0.887\,II) \tag{6}$$

$$VCG_z = -(-0.229\,V1 - 0.310\,V2 - 0.246\,V3 - 0.063\,V4 + 0.055\,V5 + 0.108\,V6 + 0.022\,I + 0.102\,II) \tag{7}$$

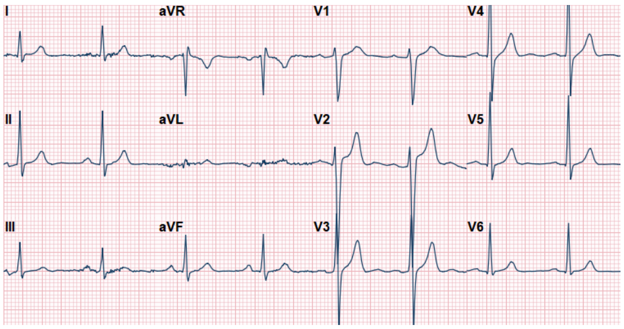

Figure 2 - Standard 12 leads ECG of the control healthy case.

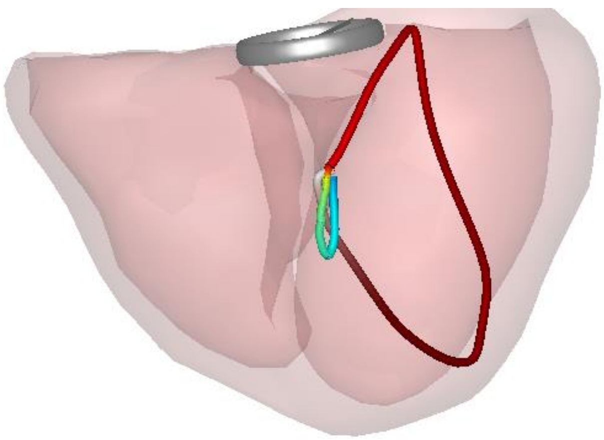

Figure 3 - VCG for the healthy control patient.

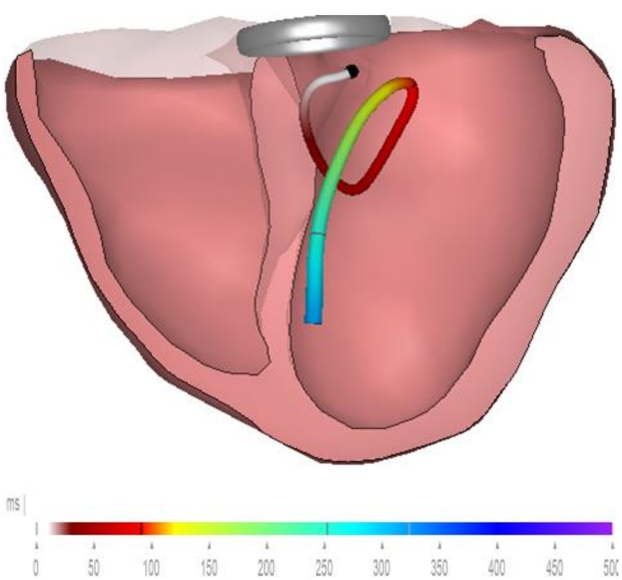

Figure 4- CineECG of the control case.

Where $(VCG_x, VCG_y, and\ VCG_z)$ are the vector component in 3D of the VCG, $I\ and\ II$ are the reading of the first and second standard limb reads, while $V1{\sim}V6$ are the readings of the precordial (Chest) leads. however, clinically VCG was not used extensively, due to complex pattern, (*ex*, using the 12 lead ECG from healthy subject shown in Figure (2) the VCG shown in Figure (3) was created, and the fact that it is described using the body axis. thus, it requires rotation to the heart axis.

Also, due the simplicity aspects of the model, *i.e.,* the fixed origin vector, it cannot fit all data, which leads to the loss of some information.

3. CineECG Methodology Review:

CineECG was first described here (Boonstra et al., 2022), as a novel clinical way to evaluate the standard 12-lead ECG by describing the average location of the anatomical center of the cells that undergoing a change on transmembrane potential at a certain point of time, *i.e.,* the cells that are simultaneously electrically activated.

To calculate these positions, three inputs are required, that are the standard 12-lead ECG, the model for the torso with the placements of the electrodes and the model of the heart. In case the models are not available, CineECG used generic models of heart and torso.

CineECG considers that the average 'velocity' of the electrical activation propagation through the heart structure is 0.7 m/s. Moreover, the mid QRS complex, the average position of the cardiac activation is located at the center of mass of the heart, and this is considered as the anchor point for the CineECG, both in time and space. Once an input is acquired, CineECG is calculated recursively, using the following steps:

1. VCG is calculated using equation 8.

$$\overrightarrow{vcg} = \sum_{n=1}^{9} L_n(t)\ a_n\left(\frac{\vec{r}_n - \vec{r}_{ref}(t)}{\|\vec{r}_n - \vec{r}_{ref}(t)\|}\right) \quad (8)$$

where L_n is the lead read, and a_n is a scaling factor. $\vec{r}_n$ a vector from the origin to the nth electrode, while

$\vec{r}_{ref}$ is a vector from the reference point to the location of CineECG at (t-1), for t = 0, reference point is the centre of mass.

2. CineECG is calculated using equation 9:

$$\overrightarrow{\text{CineECG(t)}} = \overrightarrow{\text{CineECG(t-1)}} + \text{speed}\frac{\overrightarrow{\text{VCG}}}{\|\overrightarrow{\text{VCG}}\|} \quad (9)$$

3. Calculation is repeated backword in time.

The original paper(Boonstra et al., 2022) goes in depth about the calculations and all justifications for all assumptions.

4. Cases analysis:

Using the CineECG software shown in Figure (5), we processed 12 leads ECG data acquired from two different patients and one control healthy case, the clinical cases included: LBBB, RBBB. These cases were previously diagnosed by cardiologist. While the software can process data from multiple extensions *i.e.,* (mat, ecg, pdfecg, xml, txt, inf, csv, rr, bsm, json, dcd and dcm), our data was in standard DICOM.

No preprocessing was applied outside the software as the software can perform baseline corrections and acquiring a median beat before applying the CineECG algorithm and generating the 3D visual representation.

3.1. Control case:

The case belongs to a healthy male with no known heart malfunctions, Figure (2) shows the standard 12-ECG in 4 by 3 format after performing the baseline correction.

Figure (3) shows the CineECG line generated by the software, the color gradient represents the time stamps.

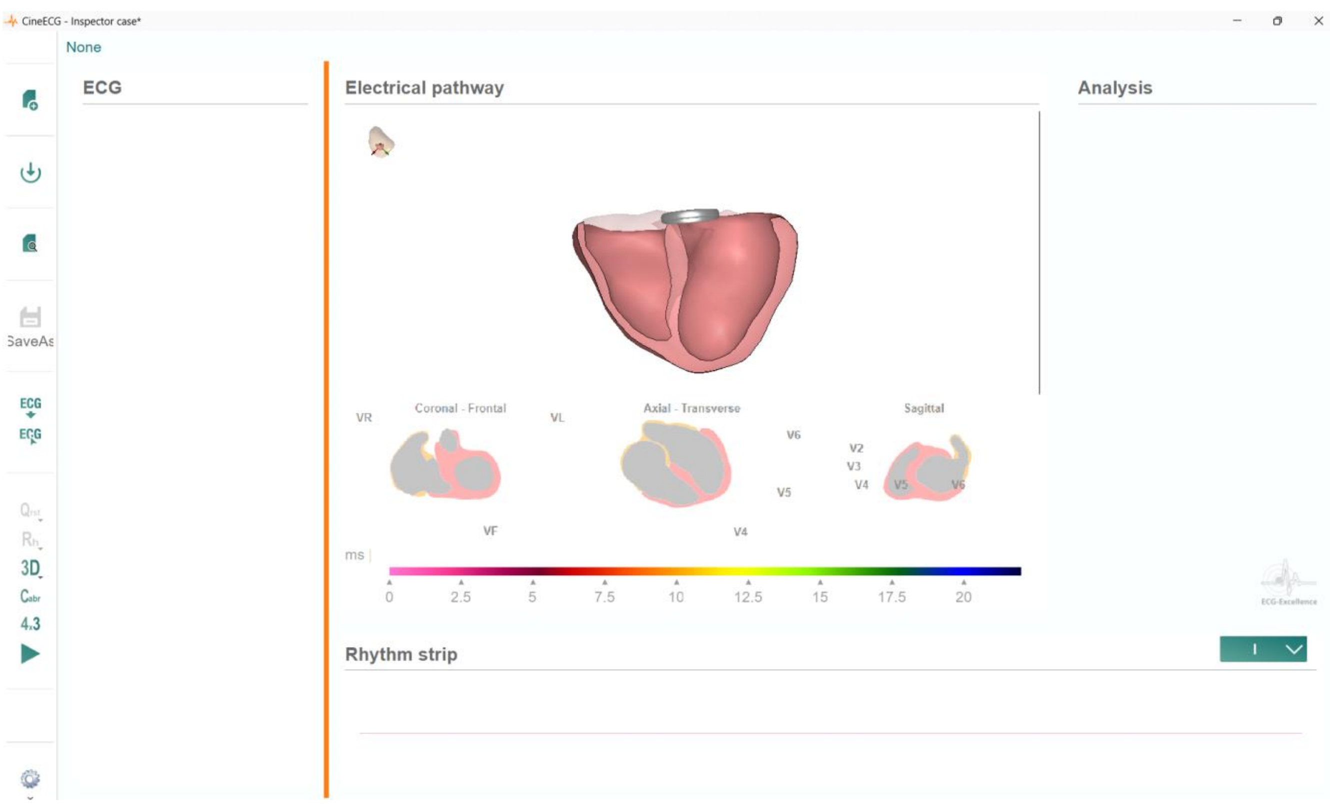

Figure 5 - CineECG user interface, with no loaded ECG.

The healthy case can be described in three phases.

a) QRS complex: the line propagates through the septum, followed by the line moving toward the apex and the left free wall, before making a turn towards the base around the R top.
b) ST segment: the vector is propagating towards the apex, with shifting to the interior and the septum.
c) T-wave: the line shows moving toward the apex.

3.2. LBBB case:

Figure (6) shows the standard 12-leads of an LBBB patient, after baseline correction, and Figure (7) shows the generated CineECG. The electrical path in the CineECG clearly differs from the normal case,

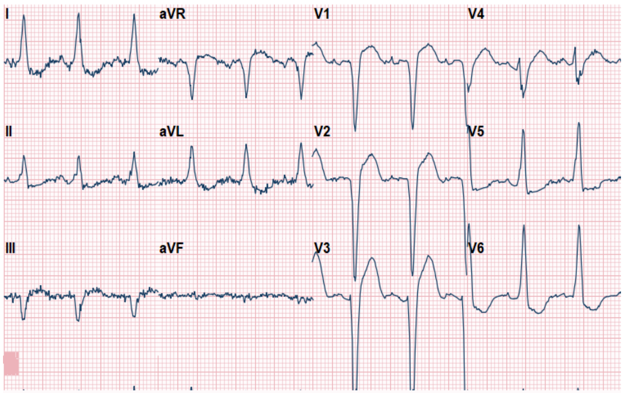

Figure 6- CineECG of the LBBB case.

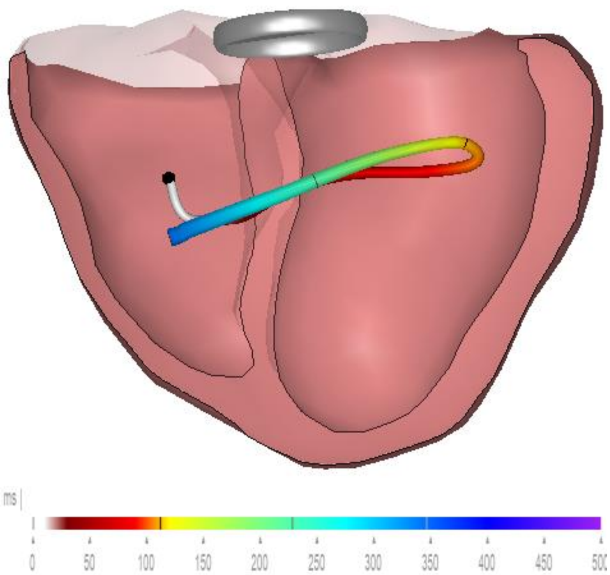

Figure 7 - CineECG of LBBB case.

and with further inspections we can see it starts from the right ventricle, travel through the septum to the left ventricle, and for the repolarization is traveling from the left ventricle to the right one.

3.3. RBBB Case:

Figure (8) shows the standard 12-leads ECG of an RBBB patient, after baseline correction while the CineECG is shown in Figure (9). Just like in LBBB case the CineECG line shows different from the normal path. In the case of RBBB, the CineECG line starts from the left ventricle followed by moving towards the right one through the septum, and then the repolarization line is traveling toward the base instead of the apex.

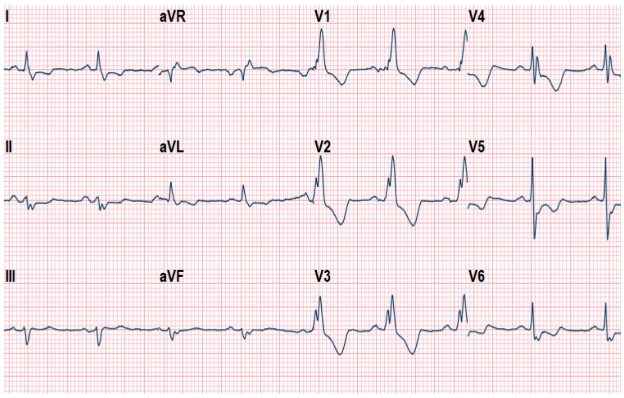

Figure 8 - Standard 12-lead ECG of the RBBB.

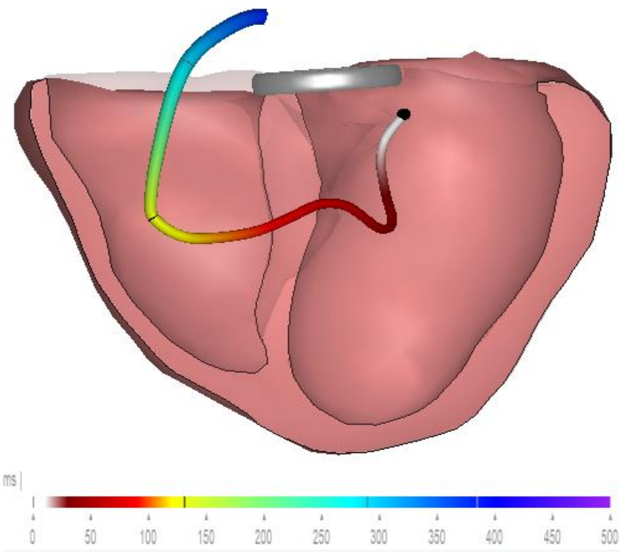

Figure 9- CineECG in case of RBBB.

5. Discussion:

The aim of the present work was to review the software CineECG, in order to demonstrate its innovative ability in supporting the clinicians in the standard 12-lead interpretation.

The control case findings agree with what we already know about the path of the electrical signal in the heart starting from the Atrioventricular (AV) Node, then down using the bundle of His, then to the left and right ventricles using the bundle branches with the line shifted toward the left ventricle because of its bigger mass comparing to the right, finally although the Repolarization travel from the apex to the base, the charge is reversed and thus it shows raveling towards the apex. This case showed a true potential for the tool as well as established a reference to be considered when examining the clinical cases.

LBBB and RBBB are diagnosed primarily by ECG where the electrical activity in the LBBB ECG shows symptoms like widened QRS complex (> 120 ms), a dominant S wave in lead V1, broad, monophasic R wave in lateral leads (I, aVL, V5-V6), and an absence of Q waves in lateral leads(Nikoo et al., 2013). While the RBBB, shows morphologies like a widened QRS complex (> 120 ms), what is known as RSR' pattern in leads V1-V3 (appearing like an "M") and a wide, slurred S wave in lateral leads (I, aVL, V5-V6)(Surawicz et al., 2009). These finding are not easy to recognise, as it may differentiate among patients, and it requires much expertise and understanding of the ECG to be diagnosed.

However using the CineECG for the LBBB case, the visual indicate a problem with the signal path moving toward the left ventricle since the right ventricle is activated before it, which agree with the diagnosis of the LBBB.

And for the RBBB case the observations agree as well with the block in the right bundle which causes the delay in the depolarization and given the fact the T-wave is reversed in this case of RBBB, that explain the inverse direction of the repolarization wave.

These cases showed the fact that the algorithm can give a good representation of the 12-Lead ECG, a representation that can be used as a diagnostic tool as well as an informatic educational tool as it describes the 12 signals with a single line,/

Limitations do exist in terms of using the generic heart and torso model, in some cases this could generate non accurate data, however, with the evaluation of auto image segmentation methods specifically the deep learning-based methods, this problem could be dealt with. In the future we look forward to quantifying these visual observations to provide better understanding and explore the ability to automate the diagnosis procedure. An educational demonstration version of CineECG, can be downloaded for free at https://cineecg.com/free-trial.

6. References:

Boonstra, M. J., Brooks, D. H., Loh, P., & van Dam, P. M. (2022). CineECG: A novel method to image the average activation sequence in the heart from the 12-lead ECG. *Computers in Biology and Medicine*, *141*, 105128. https://doi.org/https://doi.org/10.1016/j.compbiomed.2021.105128

G Daniel, G Lissa, D Medina Redondo, L Vásquez, & D Zapata. (2007). Real-time 3D vectorcardiography: an application for didactic use. *Journal of Physics: Conference Series*, *90*(1), 012013. https://doi.org/10.1088/1742-6596/90/1/012013

Ikeda, T. (2021). Right bundle branch block: current considerations. *Current Cardiology Reviews*, *17*(1), 24–30.

KORS, J. A., VAN HERPEN, G., SITTIG, A. C., & VAN BEMMEL, J. H. (1990). Reconstruction of the Frank vectorcardiogram from standard electrocardiographic leads: diagnostic comparison of different methods. *European Heart Journal*, *11*(12), 1083–1092. https://doi.org/10.1093/oxfordjournals.eurheartj.a059647

Nikoo, M. H., Aslani, A., & Jorat, M. V. (2013). LBBB: State-of-the-Art

Criteria. In *Int Cardiovasc Res J* (Vol. 7, Issue 2).

Sgarbossa, E. B. (2000). Value of the ECG in suspected acute myocardial infarction with left bundle branch block. *Journal of Electrocardiology*, *33*, 87–92.

Surawicz, B., Childers, R., Deal, B. J., & Gettes, L. S. (2009). AHA/ACCF/HRS Recommendations for the Standardization and Interpretation of the Electrocardiogram. Part III: Intraventricular Conduction Disturbances A Scientific Statement From the American Heart Association Electrocardiography and Arrhythmias Committee, Council on Clinical Cardiology; the American College of Cardiology Foundation; and the Heart Rhythm Society. In *Journal of the American College of Cardiology* (Vol. 53, Issue 11, pp. 976–981). https://doi.org/10.1016/j.jacc.2008.12.013

Thomson, D., Kourounis, G., Trenear, R., Messow, C.-M., Hrobar, P., Mackay, A., & Isles, C. (2019). ECG in suspected pulmonary embolism. *Postgraduate Medical Journal*, *95*(1119), 12–17.

Wimmer, N. J., Scirica, B. M., & Stone, P. H. (2013). The Clinical Significance of Continuous ECG (Ambulatory ECG or Holter) Monitoring of the ST-Segment to Evaluate Ischemia: A Review. *Progress in Cardiovascular Diseases*, *56*(2), 195–202. https://doi.org/https://doi.org/10.1016/j.pcad.2013.07.001